CHARACTERISTICS OF OUTPUT POWERS OF PULSED ARGON-ION LASERS IN GAS MIXTURES

Toshio GOTO, Koichi NAKAMURA and Shuzo HATTORI

Department of Electronic Engineering

(Received October 30, 1969)

Abstract

It will be interesting to study the properties of pulsed argon ion lasers by mixing helium gas with argon gas because it produces the combinations of electron temperatures and densities different from that in pure argon. In this experiment, the 4880 Å and 4765 Å relative laser powers in Ar-He gas mixtures were examined as a function of discharge current in the 6 and 10 mm bore tubes. Although the 4880 Å peak laser power decreases rapidly with the increase in discharge current at a pressure of 15 mtorr of pure argon, the different phenomena occur when the helium gas is mixed. They are interpreted qualitatively with the measured electron temperatures and densities, and with considering several formation and destruction processes for laser states.

1. Introduction

Properties of laser output pulses in pure argon excited inductively have beer described in our previous papers[1)2)3)]. Particularly, the 4880 Å and 4765 Å laser output pulses show interesting characteristics at high currents. To study the mechanism of them more minutely, it is worthwhile to vary electron temperature and density independently. For this purpose, helium gas is mixed with argon gas.

At first, singly ionized argon ion lasers were obtained in Ar-He or Ar-Ne gas mixtures[4)5)6)]. However, it was reported also that addition of buffer gas decreased the laser output power when partial pressure of helium gas became higher[7)]. Actually, the same phenomenon was observed also in our case. From the viewpoint of obtaining high power lasers, therefore, addition of helium gas is not desirable. However, it is interesting to utilize helium gas as a means to study physical properties of argon ion lasers at high currents. In a fixed laser tube and excitation method of gas, if a certain pair of argon pressure and input power are chosen, one pair of the electron temperature and density are determined. However, the combination of those values can be changed if helium gas is mixed with argon gas. If only helium gas is increased even at a constant argon pressure, the electron temperature and density will change. Since it influences on the relative importance of the excitation and destruction processes, the characteristics of saturations of the laser output powers will differ from those observed in pure argon. Actually, they were observed in our experiment. Thus, helium gas was not used to stabilize gas discharge or as buffer gas, but was utilized as a means to vary the electron temperature and density independently.

The properties of argon ion lasers in pure argon were interpreted with the measured plasma parameters and the rate equations for the laser states in which the five formation and destruction processes were considered[8]. Also in this paper, the same rate equations will be used and it will be shown that the properties of the laser output powers in helium-argon gas mixtures will be explained qualitatively by considering the influence of helium gas on the measured electron temperature and density. It also results in the verification of the rate equations.

2. Experimental

As the arrangement used in this experiment has been described in our previous paper[2], it is mentioned briefly here. A ring laser tube was used which was composed of a capillary of 6 mm in diameter and 30 cm in length, and a bypass tube of 1.6 cm in diameter. A tube of 10 mm bore also was used. They were set in the secondary of the transformer and filling gas was excited inductively by input 10 μsec pulses. A rf generator was used to facilitate the initiation of gas discharge. Discharge currents were examined with a Rogowskii coil. Laser output powers were examined with a photoelectric method. Electron temperature and density were measured with the double probe method described by Johnson and Malter[9].

The peak discharge current was in the range of 100 to 750 A. A ratio of partial pressures of Ar and He was changed in the range of 1 : 0 to 1 : 10, and also the total pressure was changed.

3. Experimental Results

Fig. 1 shows current pulses and laser output pulses for the 4880 Å and 4765 Å transitions at a pressure of 15 mtorr in the 6 mm bore tube. In this paper, for the 4880 Å transition, we examine the current and pressure dependences of the first peak P and the last peak R which appears in the 40 μsec pulse excitation. For the 4765 Å transition, only a peak P is treated.

Fig. 2 shows the P peak laser intensity of the 4880 Å transition vs peak current characteristics at three Ar-He pressures and a pressure of 15 mtorr of pure argon. The ratio of partial pressures of argon and helium is constant (1 : 10). At currents below 200 A, there are not qualitative differences between the current dependence of the laser power in pure argon and those in Ar-He gas mixtures. At currents above 200 A, however, the peak laser output power decreases with the discharge current more rapidly at higher Ar-He pressures.

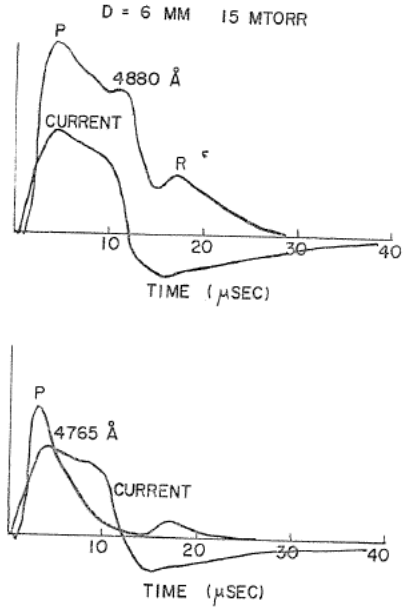

FIG. 1. Current and laser output pulses of the 4880 Å and 4765 Å transitions. Vertical: arbitrary unit, linear scale.

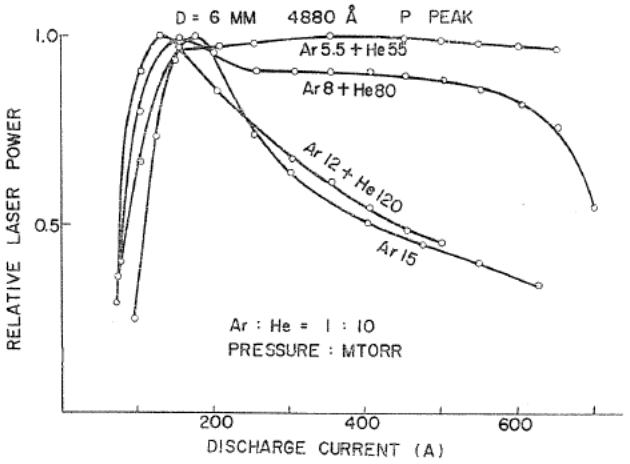

FIG. 2. *P* peak laser output power of the 4880 Å transition as a function of peak current at Ar: He=1 : 10.

At Ar-He pressures of 60.5 mtorr and 88 mtorr, the curves have flat tops and the laser powers do not show remarkable decrease. However, the absolute value of the maximum of the laser power at each pressure becomes smaller at lower Ar-He pressures.

To examine the influence of helium gas more definitely, argon pressure should be kept constant and only helium pressure should be changed. The result obtained for the 4880 Å transition is shown in Fig. 3, which has been reported in our other paper[10]. The relative laser output power decreases with the increase

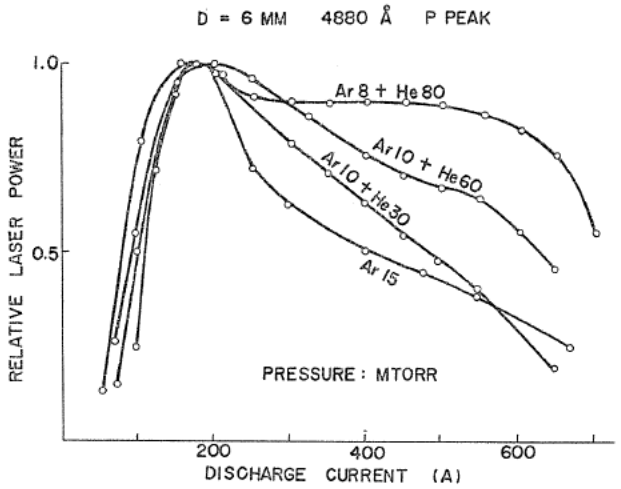

FIG. 3. *P* peak laser output power of the 4880 Å transition as a function of discharge current when only helium pressure is changed at a constant argon pressure (~10 mtorr). In the 10 mm bore tube, the same phenomenon was observed. However, the saturation occurred at a current of about 800 A.

in discharge current more slowly as helium pressure becomes higher. However, the absolute value of the maximum of the laser output power decreases with the increase in helium pressure. Also in the 10 mm bore tube, the same phenomenon was observed but the current at which the laser output power was saturated was about 800 A.

The result for the 4765 Å transition is shown in Fig. 4. Both the threshold current and the current at which saturation occurs increase with the increase in helium pressure. The absolute laser output power is smaller at higher helium pressures. In the 10 mm bore tube, the saturation did not occur even at currents above 1000 A. For the 4880 Å transition, thus, the difference occurs at currents above the saturation current, but for the 4765 Å transition, the saturation current itself changes remarkably.

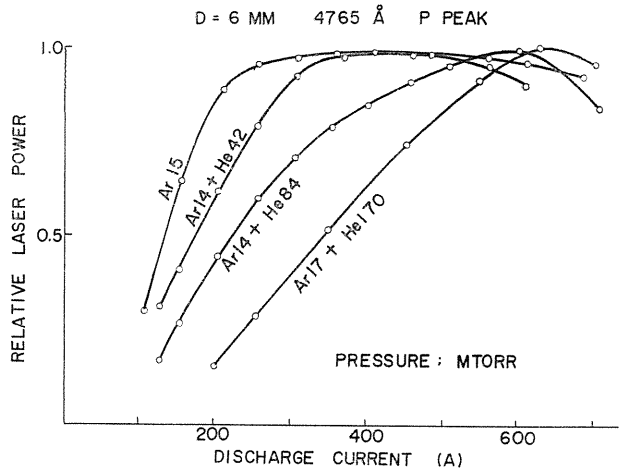

FIG. 4. *P* peak laser output power of the 4765 Å transition as a function of discharge current when only helium pressure is changed at a constant argon pressure (~14 mtorr). In the 10 mm bore tube, the laser output power was not saturated even at currents above 1000 A.

Fig. 5 shows *R* peak laser power vs peak current characteristics for the 4880 Å transition. In helium-argon gas mixtures, the threshold current is higher than in pure argon and the rate of increase in laser output power is smaller. The saturaion does not occur even at currents above 300 A. In the 10 mm bore tube, the peak *R* did not appear.

Next, the electron temperature and density necessary for the understanding of the mechanism of argon ion lasers were measured with the double probe method. The measurements were made on the tube axis in the 6 mm bore tube and at the position of 3 mm away from the tube axis in the 10 mm bore tube. The result is shown in Fig. 6. It is partially on account of the position that the electron temperatures in the two tubes are more different than those in pure argon which the measurements were made at the same positions[5]. At a pressure of 15 mtorr of pure argon, the electron temperature increases from 8×10^4 to

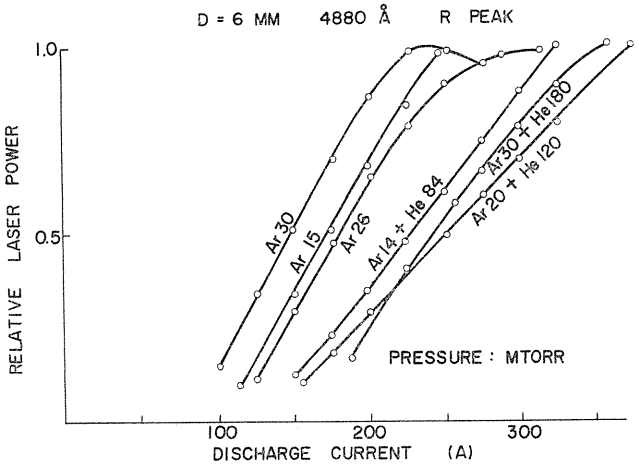

FIG. 5. R peak laser output power of the 4880 Å transition as a function of peak current at several pressures. In the 10 mm bore tube, the R peak did not appear.

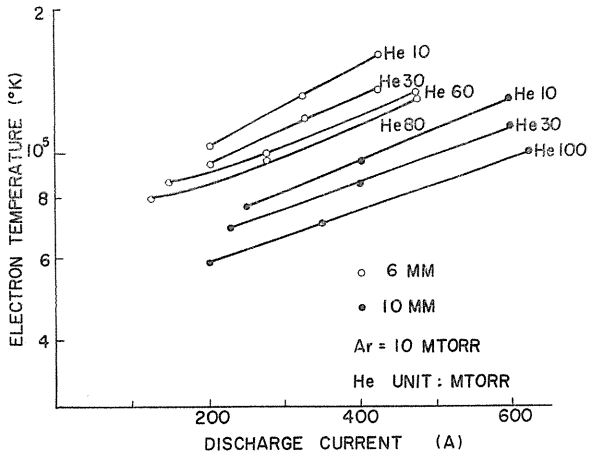

FIG. 6. Peak electron temperature as a function of peak discharge current in the 6 and 10 mm bore tube.

10^{5}°K when the discharge current increases from 100 to 500 A in the 6 mm bore tube[8]. Fig. 6 shows that the electron temperatures in gas mixtures are higher than that in pure argon. As inferred from the Tonks-Langmuir's relation[11], the electron temperature in pure helium is much higher than in pure argon. The measured values seem to be intermediate ones determined by partial pressures of the two gases. The increase in electron temperature with rising currents was observed also in these gas mixtures. Although the error in low current regions is 10–15%, the exact measurement is difficult on account of fluctuation in probe current at currents above 450 A. Therefore, that result is not shown in the figure.

Fig. 7 shows the peak electron density as a function of peak discharge current.

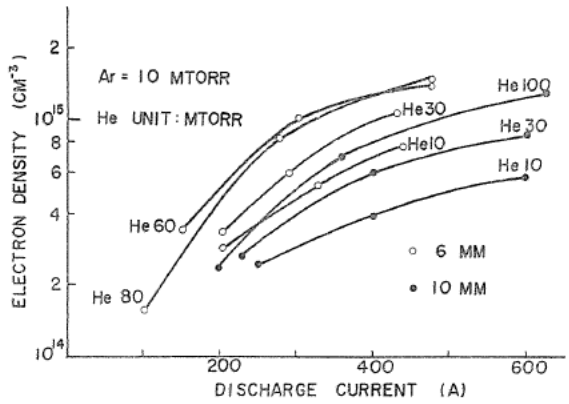

FIG. 7. Peak electron density as a function of peak discharge current in the 6 and 10 mm bore tube.

At a pressure of 15 mtorr of pure argon in the 6 mm bore tube, it increases from 2×10^{14} to 10^{15} cm^{-3} when the discharge current increases from 100 to 550 A. The large value is due to the pinch effect and double ionization. However, the electron density does not increase very much even if helium gas is mixed. It is because the ionization potential of helium is high and the total ionization cross section is about one order of magnitude smaller than that of argon[12].

4. Discussions

It is the following processes that we must take into account for the populations of upper and lower states of argon ion lasers. The ionic excited states are formed by the singlestep process from the neutral ground state, the multistep process through the ion ground state, and the cascade transitions from the higher states. They decay on account of radiation and electron collisions. At the steady state, equations for the populations of the upper and lower levels 2 and 1 of the argon ion laser are given by

$$S_2 n_{0A} n_e + M_2 n_{iA} n_e + \sum A_{j2} n_j - A_2 n_2 - D_2 n_2 n_e = 0 \tag{1}$$

$$S_1 n_{0A} n_e + M_1 n_{iA} n_e + \sum A_{j1} n_j - F A_1 n_1 - D_1 n_1 n_e = 0, \tag{2}$$

where S and M are the formation rates by the singlestep and multistep excitations, respectively. A and D are the destruction rates by the radiation and electron collisions, respectively. $\sum A_{j2} n_j$ and $\sum A_{j1} n_j$ represent the contributions of the cascade effects. n_{0A} and n_{iA} are the argon neutral atom and argon ion densities, respectively. $n_e = n_{eH} + n_{eA}$, where n_{eH} and n_{eA} are the densities of the electrons formed by the ionizations of the argon and helium atoms, respectively. Therefore, $n_{iA} = n_{eA}$. F in equation (2) shows the radiation trapping effect. When the Doppler broadening is dominant and the tube is cylindrical, $F = C/k_0 R(\log k_0 R)^{1/2}$ [13], where k_0 is the absorption coefficient, R is the tube radius and C is a constant.

Since $k_0 R$ is relatively large in our case, for simplicity, we assume that $F \propto (k_0 R)^{-1}$ and put $F = \Delta\nu_D'/n_{iA}K$, where $\Delta\nu_D'$ is the Doppler width of the resonance line (720 Å). Moreover, it is assumed that $\sum_j A_{j2} n_j = r_2 A_2 n_2$ and $\sum_j A_{j1} n_1 = r_1 F A_1 n_1$.

Then, the quantity $P=\{n_2-(g_2/g_1)n_1\}1/\Delta\nu_D-f$ which is approximately proportional to the laser output power is obtained from the equations (1) and (2), where f represents the loss term and $\Delta\nu_D$ is the Doppler width of the laser transition. Here, we simplify the expression P with very rough approximation to be able to examine easily how P depends on the ion and electron densities.

At small n_e, the destruction terms by electron collisions are neglected. Then,

$$P_1=\{A+(B-C)n_{iA}-Dn_{iA}^2\}\frac{n_{eA}+n_{eH}}{\Delta\nu_D}-f, \tag{3}$$

where

$$\begin{aligned} A&=\frac{S_2n_{0A}}{A_2(1-r_2)} & B&=\frac{M_2}{A_2(1-r_2)} \\ C&=\frac{g_2}{g_1}\frac{KS_1n_{0A}}{A_1(1-r_1)\Delta\nu_D'} & D&=\frac{g_2}{g_1}\frac{KM_1}{A_1(1-r_1)\Delta\nu_D'}. \end{aligned} \tag{4}$$

At relatively large n_e, the radiative decay and cascade transition terms are neglected. Then,

$$P_2=(E+Fn_{iA})\frac{1}{\Delta\nu_D}-f, \tag{5}$$

where

$$E=\left(\frac{S_2}{D_2}-\frac{g_2}{g_1}\frac{S_1}{D_1}\right)n_{0A} \qquad F=\frac{M_2}{D_2}-\frac{g_2}{g_1}\frac{M_1}{D_1}. \tag{6}$$

The function $A+(B-C)n_{iA}-Dn_{iA}^2$ has the maximum at $n_{iA}=(B-C)/2D$. On the other hand, $n_{eA}+n_{eH}$ is a monotonically increasing function with the discharge current as seen in Fig. 7. Therefore, P_2 is the function which has the maximum at a certain discharge current. On the other hand, the excitation function for $4p-3p^5$ transition has a strong resonance only close to threshold and is very small in other energy regions. That for $4s-3p^5$ transition is large in rather wide energy regions[14]. Therefore, as far as the optimum electron temperature and density do not exist, perhaps $M_2/D_2<g_2M_1/g_1D_1$. Then, P_2 represented by the equation (5) is a monotonically decreasing function.

We denote by $f(n_e, T_e, v)$ the electron energy distribution which is assumed to be Maxwellian, and by σ_A and σ_H the total ionization cross sections of argon and helium, respectively. Then, the rate of ionization depends on $\int n_0\sigma n_e f(n_e, T_e, v)vdv$. The change of T_e influences n_{iA}, n_{iH}, n_{eA} and n_{eH} as follows. If $T_{e1}<T_{e2}$ and $v_1<v_2$,

$$\frac{f(n_{e1}, T_{e1}, v_2)}{f(n_{e1}, T_{e1}, v_1)}<\frac{f(n_{e2}, T_{e2}, v_2)}{f(n_{e2}, T_{e2}, v_1)}. \tag{7}$$

When the electron energy increases from 30 to 100 eV, σ_H/σ_A increases from 0.037 to 0.13[12]. Therefore,

$$\frac{n_{iH}(T_{e2})}{n_{iH}(T_{e1})}>\frac{n_{iA}(T_{e2})}{n_{iA}(T_{e1})}. \tag{8}$$

That is,

$$\frac{n_{eH}(T_{e2})}{n_{eA}(T_{e2})} > \frac{n_{eH}(T_{e1})}{n_{eA}(T_{e1})}. \tag{9}$$

There is not information for the excitation cross sections of the laser lower and upper states enough to interprete quantitatively the laser output power characteristics. It is the single-step excitation cross sections of the $4p$ states that have been investigated[15)16)17)]. In this paper, therefore, the results in Figs. 2, 3, 4 and 5 are discussed merely qualitatively on the basis of the equations (3)–(9) and the measured electron temperature and density.

Fig. 2 shows that saturation of the 4880 Å laser output power occurs at a current of about 150 A. However, the electron density at that current is larger at higher Ar-He pressures. As seen in Fig. 6, T_e increases and $n_e = n_{iA} + n_{iH}$ decreases with the decrease in Ar-He pressure. If $J_2 > J_1$ and $p_2 > p_1$, $n_e(J_2, p_1) - n_e(J_1, p_1) < n_e(J_2, p_2) - n_e(J_1, p_2)$, where J and p are the current density and gas pressure, respectively. It is found from the equations (8) and (9) that n_{iA}/n_e decreases. Therefore, $n_{iA}(J_2, p_1) - n_{iA}(J_1, p_1) < n_{iA}(J_2, p_2) - n_{iA}(J_1, p_2)$. It shows that P_1 decreases more rapidly at higher pressures as the discharge current becomes higher than 150 A. Moreover, since T_e is higher at lower pressures, the relative importance of S increases and therefore A does. Perhaps it also is one cause of behavior in Fig. 2. When the change of n_{iA} with the discharge current is small, P_2 also does not change very remarkably. Consequently, the 4880 Å laser output power decreases more slowly with the discharge current at higher Ar-He pressures.

Fig. 3 shows that the 4880 Å laser output power decreases more slowly with the discharge current as helium pressure becomes higher. Since T_e changes with the increase in helium pressure, the coefficients A, B, C, and D change. However, since argon pressure is constant, $n_{iA}(J, p_{H2})$ is not so different from $n_{iA}(J, p_{H1})$ as when argon pressure changes. Therefore, $A + (B - C)n_{iA} - Dn_{iA}^2$ does not differ very much at two helium pressures. On the other hand, as shown in Fig. 7, n_e increases more rapidly at higher helium pressures. Since P_1 is the product of the two factors, the rate of decrease in P_1 with the discharge current becomes smaller at higher helium pressures.

In Fig. 5, the laser output power vs discharge current curves in Ar-He gas mixtures exist in higher current regions than those in pure argon. The electron density in the 40 μsec pulse excitation is smaller than in the 10 μsec pulse excitation. It is supposed, therefore, that n_{iA} does not amount to the value necessary for saturation of the laser output power even at a current of 350 A in Ar-He gas mixtures.

As seen in Fig. 4, the 4765 Å laser output power shows the characteristic different from the 4880 Å one. Although there is not the exact information about M_1, M_2, and S_1, perhaps the difference of the characteristics for the two transitions is due to that of the excitation cross section for each state. The relative importance of S_1 may decrease fairly rapidly for the 4765 Å transition when T_e decreases with the increase in helium gas. Then, since C becomes smaller, the saturation point moves to the higher current region.

In the above discussion, for simplicity, the changes of the neutral atom density, cascade rate, and Doppler width were neglected.

5. Conclusions

The current dependences of the peak laser powers in Ar-He gas mixtures are different from those in pure argon. However, the properties are to some extent interpreted with using the rate equations similar to those in pure argon and with considering the changes of electron temperature and density by mixture of helium. Those two parameters seem to have very important influence on the laser output powers.

Acknowledgment

The authors wish to express their thanks to S. Chinen for his assistance in this experiment.

References

1) S. Hattori and T. Goto, Appl. Phys. Letters, **12**, 131 (1968).
2) S. Hattori and T. Goto, J. Appl. Phys., **39**, 5998 (1968).
3) S. Hattori and T. Goto, Japa. J. Appl. Phys., **8**, 1159 (1969).
4) W. B. Brigdes, Appl. Phys. Letters, **4**, 128 (1964).
5) Convert, G., Armand, M., and Martinot-Lagarde, P., Compt. Rend. Acad. Sci. Paris, **258**, 3259 (1964).
6) H. G. Heard, G. Makhov and J. Peteraon, Proc. IEEE, **52**, 414 (1964).
7) W. R. Bennett, Jr., J. W. Knutson, Jr., G. N. Mercer and J. L. Detch, Appl. Phys. Letters, **4**, 180 (1964).
8) S. Hattori and T. Goto, IEEE J. Quantum Electronics **QE-5**, No. 11 (1969).
9) E. O. Johnson and L. Malter, Phys. Rev., **80**, 58 (1950).
10) T. Goto, K. Nakamura and S. Hattori, IEEE J. Quantum Electronics, QE-6. No. 3 (1970).
11) L. Tonks and I. Langmuir, Phys. Rev. **34**, 876 (1929).
12) D. Rapp and P. Englander-Golden, J. Chem. Phys., **43**, 1464 (1965).
13) T. Holstein, Phys. Rev., **72**, 1212 (1947).
14) W. R. Bennett, Jr., Appl. Optics Suppl., **2**, 3 (1965).
15) S. H. Koozekanani, IEEE J. Quantum Electronics **QE-2**, 770 (1966).
16) W. R. Bennett, Jr., G. N. Mercer, P. J. Kindlmann, B. Wexler and H. Hyman, Phys. Rev. Letters, **17**, 987 (1966).
17) J. M. Hammer and C. P. Wen, J. Chem. Phys., **46**, 1225 (1967).